

The black hole–bulge relation in AGNs

W. Bian^{1,2*} and Y. Zhao¹

¹*National Astronomical Observatories, Chinese Academy of Sciences, Beijing 100012, China*

²*Department of Physics, Nanjing Normal University, Nanjing 210097, China*

ABSTRACT

We used the widths of H β and [OIII] emission lines to investigate the black hole–bulge relation in radio-loud AGNs, radio-quiet AGNs and NLS1s. The central black hole mass, M_{bh} , is estimated from the H β line width and the optical luminosity, and the bulge velocity dispersion, σ , is directly from the width of [OIII] line. We found that the radio-quiet AGNs follow the established $M_{bh} - \sigma$ relationship in nearby inactive galaxies, while the radio-loud AGNs and NLS1s deviate from this relationship. There are two plausible interpretations for the deviation of radio-loud AGNs. One is that the size of broad line regions (BLRs) emitting H β line is overestimated because of the overestimation of optical luminosity, the other is that the dynamics of BLRs and/or narrow line regions (NLRs) in radio-loud AGNs is different from that in radio-quiet AGNs. The deviation of NLS1s may be due to the small inclination of BLRs to the line of sight or the reliability of [OIII] line width as the indicator of stellar velocity dispersion because of its complex multiple components.

Key words: black hole physics — galaxies: active — galaxies: nuclei — quasars: general.

1 INTRODUCTION

Evidence shows that the evolution of black holes and that of their host galaxies appear to be closely coupled. It was found that there is strong correlation between the central black hole masses, M_{bh} , and their bulge stellar velocity dispersion, σ . Tremaine et al. (2002) investigated this relationship in a sample of 31 nearby inactive galaxies and gave a better expression as,

$$M_{bh} = 10^{8.13} (\sigma / (200 \text{ km s}^{-1}))^{4.02} M_{\odot}, \quad (1)$$

There are many methods to estimate the central black hole masses (Bian & Zhao 2003a and reference therein). In these methods, the reverberation method is thought to be more reliable. Using the reverberation mapping method, the sizes of broad line regions (BLRs) and then the central black hole masses were obtained for 37 AGNs (Ho 1998; Wandel et al. 1999; Kaspi et al. 2000). For some AGNs with available bulge velocity dispersion and the reverberation mapping mass, Gebhardt et al. (2000) and Ferrarese et al. (2001) also found that these AGNs also follow the $M_{bh} - \sigma$ relation founded in the nearby inactive galaxies. As we know, it is difficult to obtain the bulge velocity dispersion of AGNs. In order to investigate this relation in a larger sample of AGNs, Nelson (2000) used the width of [OIII] line emitting from the narrow line region (NLRs) to indicate the bulge

velocity dispersion, where $\sigma = FWHM([OIII])/2.35$, and found that these 37 AGNs with the reverberation mapping masses follow the $M_{bh} - \sigma$ relation. Wang & Lu (2001) investigated this relation in a sample of NLS1s from Veron-Cetty & Veron (2001). They used the B band magnitude and the H β FWHM to estimate the black hole masses and the [OIII] FWHM to indicate the bulge velocity dispersion. They found that NLS1s also follow the $M_{bh} - \sigma$ relation but with more scatter. We should notice that NLS1s deviated from the correlation defined in the nearby inactive galaxies if we think [OIII] FWHM is not overestimated because of the spectral resolution. Using the Sloan Digital Sky Survey (SDSS), Boroson (2003) investigated the relation between the black hole mass via the H β FWHM and the stellar velocity dispersion via [OIII] FWHM in a sample of 107 low-redshift radio-quiet AGNs. They found the correlation is consistent with that defined in nearby galaxies and the [OIII] FWHM can predict black hole mass to a factor of 5. There are only a few radio-loud AGNs in Boroson (2003). Shields et al. (2003) also investigated the $M_{bh} - \sigma$ relation as a function of redshift for an assembled sample of quasars. They suggested that this correlation can be right out to redshift of $z \approx 3$. However, Shields et al. (2003) noticed that the radio-loud AGNs seem to deviate from this correlation.

The central black hole mass can be obtained from the H β FWHM and the optical luminosity, and the bulge velocity dispersion can be indicated by the [OIII] FWHM. This provides us the opportunity to investigate the $M_{bh} - \sigma$ re-

* E-mail: whbian@njnu.edu.cn

lation in a larger sample of AGNs with available optical spectra. Moreover, we need to investigate this correlation in a larger sample of radio-loud AGNs and NLS1s. In next section we present the method to estimate the black hole mass, and then our adopted data set. Our results and discussion are given in section 3. Conclusion is presented in the last section. All of the cosmological calculations in this paper assume $H_0 = 75 \text{ km s}^{-1} \text{ Mpc}^{-1}$, $\Omega_M = 0.3$, $\Omega_\Lambda = 0.7$.

2 METHOD AND DATA

2.1 Estimation the Black Hole Masses

For the reverberation mapping method, it takes a long-term to simultaneously monitor the variability of the broad emission line and the continuum, and then to obtain the BLRs size. Up to now, there are only 37 AGNs with the reverberation mapping mass (Ho 1998; Wandel et al. 1999; Kaspi et al 2000). Fortunately, with the study of the reverberation mapping method, Kaspi et al. (2000) found an empirical correlation between the BLRs size and the monochromatic luminosity at 5100\AA :

$$R_{\text{BLR}} = 32.9 \left(\frac{\lambda L_\lambda(5100\text{\AA})}{10^{44} \text{erg} \cdot \text{s}^{-1}} \right)^{0.7} \text{ lt} - \text{days}, \quad (2)$$

where $\lambda L_\lambda(5100\text{\AA})$ can be estimated from the optical magnitude by adopting an average optical spectral index of -0.3 and accounting for Galactic reddening and K-correction (Wang & Lu 2001). Assuming that the $H\beta$ widths reflect the Keplerian velocity of the line-emitting BLR material around the central black hole, we can estimate the viral black hole mass:

$$M_{\text{bh}} = R_{\text{BLR}} V^2 G^{-1}, \quad (3)$$

where G is the gravitational constant, V is the velocity of the line-emitting material. V can be derived from FWHM of the $H\beta$ width. Assuming the random orbits, Kaspi et al.(2000) related V to FWHM of $H\beta$ line by $V = (\sqrt{3}/2)\text{FWHM}_{[H\beta]}$.

This method to estimate the central black hole masses of AGNs has been discussed by some authors (Wang & Lu 2001; Bian & Zhao 2003b; Bian & Zhao 2003c; Shields et al. 2003; Boroson 2003).

2.2 Data of NLS1s

Williams et al. (2003) presented a sample of 150 low-redshift NLS1s ($z < 0.8$) found within the SDSS. Using the SDSS Query Tool, we downloaded the spectra data and the photometry data of these 150 NLS1s. We used the $H\beta$ FWHM from their Table 1. The value of $\lambda L_\lambda(5100\text{\AA})$ is estimated from the r^* magnitude. Fluxes were converted to luminosity using the Schlegel et al.(1998) maps for correcting for Galactic absorption. We can obtain the central black hole masses in these 150 NLS1s through equation (2) and (3). Each spectrum was shifted to the rest frame and we performed a quadratic continuum fit. Using the splot tools in IRAF software, We measured the [OIII] FWHM through a Gaussian curve fit to each [OIII] line. The spectrum resolution R is about 1800, which is equivalent to 166 km s^{-1} . The error of measured [OIII] FWHM and $H\beta$ FWHM is about 10%. The [OIII] FWHM is used to estimate the host velocity

dispersion. It is difficult to measure [OIII] FWHM in three NLS1s of SDSS J010226.31-003904.6, SDSS J013521.68 - 004402.2, and SDSS J15324.367-004342.5 because of their [OIII] line with irregular profile or low signal-noise ratio, which are omitted in our discussion. We listed the NLS1s data in Table 1.

2.3 Data of Radio-Loud and Radio-Quiet AGNs

For radio-loud and radio-quiet AGNs, we adopted the data of the widths of $H\beta$ line and [OIII] line from Marziani et al. (1996). Marziani et al. (1996) used a sample of 52 low-redshift ($z < 0.8$) AGNs with available UV and optical spectra to do a comparative analysis of high-ionization and low-ionization lines in BLRs. There are 31 radio-loud AGNs and 21 radio-quiet AGNs in their sample. They found radio-loud and radio-quiet AGNs show strong difference on the dynamic of emission lines in BLRs. The sample is suitable to study the difference if any on $M_{\text{bh}} - \sigma$ relation between radio-loud and radio-quiet AGNs. For FWHM of broad component of $H\beta$ line, FeII emission and the narrow component were subtracted. We obtained FWHM of $H\beta$ line from Column (10) and (12) in Table 8 from Marziani et al. (1996). The absolute optical B band magnitude for these 52 AGNs are adopted from Veron-Cetty & Veron (2001). The [OIII] line widths are adopted from Column (17) in Table 5 from Marziani et al. (1996). There are 48 AGNs with available widths of $H\beta$ and [OIII] line. Using equation (2) and (3), we obtained the central black hole masses of 48 AGNs in the sample of Marziani et al. (1996), including 12 flat-spectrum AGNs, 18 steep-spectrum AGNs, 18 radio-quiet AGNs. The date are listed in Table 2.

3 RESULTS AND DISCUSSION

3.1 $M_{H\beta} - \sigma_{[OIII]}$ Relation

In Fig. 1 and Fig. 2, we plot black hole masses estimated from the $H\beta$ line width versus the bulge velocity dispersion obtained from the [OIII] line width for the samples of Marziani et al. (1996), Shields et al. (2003), Wang & Lu (2001), Nelson (2001), Boroson (2003), and Williams et al. (2003).

The sample of Shields et al. (2003) included 49 radio-quiet AGNs and 35 radio-loud AGNs. Shields et al. (2003) used the $H\beta$ emission line width to investigate the $M_{\text{bh}} - \sigma$ relation as a function of redshift for an assembled sample of quasars. They suggested that this correlation is not a function of redshift and can be right out to redshift of $z \approx 3$. They adopted the relation between BLRs sizes and continuum luminosity suggested by photoionization model, $R \propto L^{0.5}$. In order to consistent with our calculation, we recalculated the black hole masses of AGNs in their sample using the equation (2) and (3). The sample of Wang & Lu (2001) consisted of 59 NLS1s from Veron-Cetty et al. (2001). The sample of Williams et al. (2003) included 147 NLS1s from SDSS. Up to now, this is the largest sample of NLS1s.

From Fig. 1 and Fig. 2, it is found that radio-quiet AGNs in Marziani et al. (1996), Shields et al. (2003), and

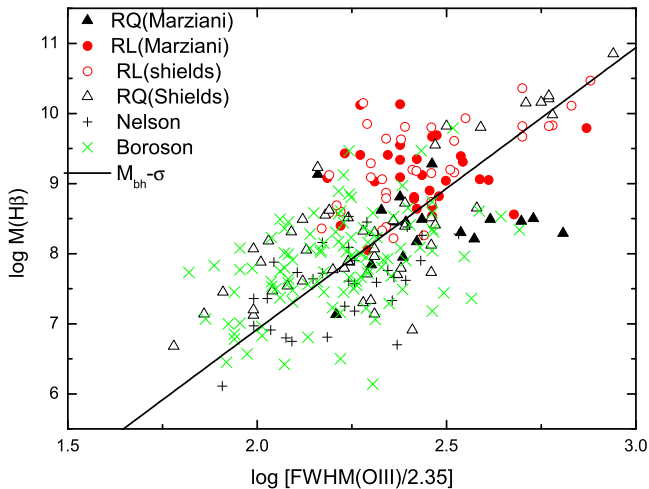


Figure 1. Black hole masses derived from $H\beta$ line width and B band magnitude versus width of the [OIII] line for AGNs. The solid line shows the $M_{\text{bh}} - \sigma$ relation from equation (1). Open circle: radio-quiet AGNs in Shields et al. (2003); solid circle: radio-loud AGNs in Shields et al. (2003); solid triangle: radio-loud AGNs from Marziani et al. (1996); open triangle: radio-quiet AGNs from Marziani et al. (1996); plus: AGNs from Nelson (2001); fork: AGNs from Boroson (2003).

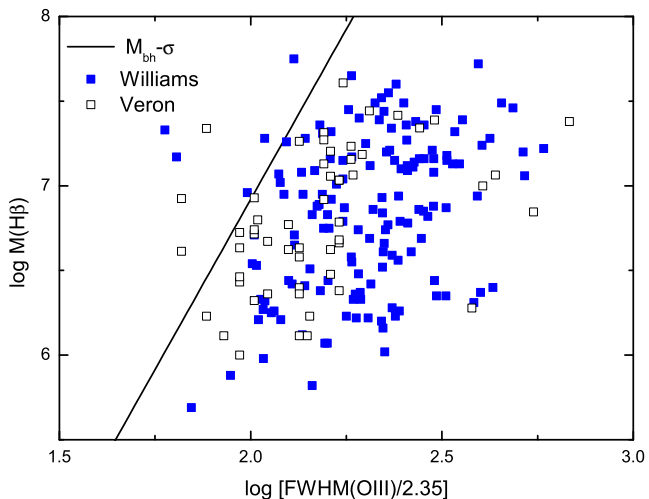


Figure 2. Black hole masses derived from $H\beta$ line width and B band magnitude versus width of the [OIII] line for Narrow-line AGNs. The solid line shows the $M_{\text{bh}} - \sigma$ relation from equation (1). Open square: NLS1s from Wang & Lu (2001); solid square: NLS1s from Williams et al. (2003).

Boroson (2003) follow the $M_{\text{bh}} - \sigma$ relation defined in equation (1) with a larger scatter compared with that in Nelson (2001). However, the radio-loud AGNs in Marziani et al. (1996) and Shields et al. (2003), and NLS1s in Wang & Lu (2001) and Williams et al. (2003) seemed not follow this relation.

For radio-loud AGNs, the mean black hole mass estimated from $H\beta$ FWHM is larger than that from [OIII] FWHM. For NLS1s, the mean black hole mass estimated from $H\beta$ FWHM is smaller than that from [OIII] FWHM. In Fig. 1 and Fig. 2, it is clear that radio-loud AGNs and NLS1s deviated from the relation defined in equation (1).

We also calculated the black hole mass, $M_{[\text{OIII}]}$, directly from the equation (1) using [OIII] line width as the indicator of σ . Table 3 showed the distribution of $\log(M_{H\beta}/M_{[\text{OIII}]})$ for different AGNs samples. The distribution of $\log(M_{H\beta}/M_{[\text{OIII}]})$ for radio-quiet AGNs in Marziani et al. (1996) is -0.36 ± 0.19 with a standard deviation of 0.81 (See Table 3). It showed that the mass estimated from $H\beta$ line width is consistent with that from the [OIII] line width but with a large scatter, which is consistent with the data of radio-quiet AGNs in Fig.1. However, the distribution of $\log(M_{H\beta}/M_{[\text{OIII}]})$ for radio-loud AGNs in Marziani et al. (2003) is 0.51 ± 0.13 with a standard deviation of 0.73. It showed that the mass estimated from $H\beta$ line width is larger than that from the [OIII] line width, which is also consistent with the data of radio-loud AGNs in Fig.1. The distributions of $\log(M_{H\beta}/M_{[\text{OIII}]})$ for radio-loud and radio-quiet AGNs in Shields et al. (2003) are listed in Table 3. The results for the sample of Shields et al. (2003) are consistent with that for the sample of Marziani et al. (1996).

3.2 Uncertainties of Black Hole Mass and Stellar Velocity Dispersion

In our analysis, we used equations (2)-(3) to calculate the black hole masses and FWHM of [OIII] line to indicate the bulge velocity dispersion. The errors of the calculated black hole masses using equations (2)-(3) are mainly from the accuracy of equation (2)-(3); the geometry and the dynamics of the BLRs, especially the disk inclination to the line of sight in NLS1s (Bian & Zhao 2002) and in flat-spectrum quasars (Jarvis & McLure 2003). The appropriate measurement of $H\beta$ line width for estimating the black hole mass were discussed by some authors (Vestergaard 2002; Shields et al. 2003). The error in the mass estimation using equations (2) and (3) is about 0.5 dex (Wang & Lu 2001).

It is possible to measure the luminosity at 5100\AA (L_{spec}) for 147 SDSS NLS1s spectrum. We compared the luminosity at 5100\AA estimated from r^* (L_r) with that from SDSS spectrum in Fig. 3. They are consistent and the distribution of $\log(L_r/L_{\text{spec}})$ is 0.21 ± 0.01 with a standard deviation of 0.15. The mean mass estimation using L_r would be enhanced by 0.15 dex compared with that using L_{spec} .

McLure & Dunlop (2001) suggested that the assumption of random orbits of BLRs seems unrealistic for quasars, and that the BLRs velocity should be related to FWHM of $H\beta$ as $V = 1.5 \times \text{FWHM}_{[H\beta]}$. It is equivalent to assume smaller inclination in quasars (see a detail discussion in McLure & Dunlop 2001). Gu et al. (2001) also used $V = 1.5 \times \text{FWHM}_{[H\beta]}$ to estimate the velocity of BLRs in

radio-loud AGNs. Jarvis & McLure (2002) investigated the relation between the black hole mass and radio luminosity in flat-spectrum quasars. Considering the Doppler boosting correction of the radio luminosity and the inclination correction of the BLRs velocity, they found flat-spectrum quasars follow the relation between radio luminosity and black hole mass found by Dunlop et al. (2003). Jarvis & McLure (2002) adopted a correction factor of two for the BLRs velocity of flat-spectrum quasars as the effect of inclination, which would increase the black hole mass estimates by a factor of four, ~ 0.6 (*dex*). Smaller inclination in radio-loud AGNs would enhance the value of BLRs virial velocity derived from $H\beta$ line width and would make radio-loud AGNs deviate much from the line defined by equation (1) in Fig.1.

The [OIII] line width may be overestimated by a factor of 1.3 because of the poor resolution spectrum (Veilleux 1991; Wang & Lu 2001). Considering the overestimation of the width of [OIII] line, we found that NLS1s in Wang & Lu (2001) and SDSS NLS1s are also deviated from the relation defined in equation (1) (see Fig. 2). The overestimation of bulge velocity dispersion derived from the observed [OIII] line width would also make radio-loud AGNs deviate much from the line defined in equation (1).

Radio-loud AGNs with significant $H\beta$ blueshifts or redshifts have been observed (Marziani et al. 1996). The over-simple models involving pure rotation or radial motion are unlikely. There are many possible components of motion in the BLRs (Marziani et al. 1996). For luminous AGNs, bright emission lines would contribute to the optical continuum luminosity, which would overestimate the BLRs sizes derived from equation (2). It's the use of a broad band luminosity (optical magnitude) not being converted to the luminosity in 5100 Å properly that also accounts for the overestimate of BLRs sizes (also see Fig. 3). The optical luminosity may be contaminated by the synchrotron emission from the jet for flat-spectrum quasars whose radio emission is beamed to us (Gu et al. 2001, Jarvis & McLure 2002). The over-estimated optical continuum luminosity would overestimate BLRs sizes, which would account for the overestimated black hole masses in radio-loud AGNs. This would lead to the deviation from the relation defined in equation (1) for radio-loud AGNs. If we think all type of galaxies follow the same $M_{\text{bh}} - \sigma$ correlation, we should be cautious to use equation (2)-(3) to calculate the black hole masses for radio-loud AGNs.

The overestimation of [OIII] FWHM from poor resolution spectrum in NLS1s is about a factor of 1.3, which would lead to about 0.4 dex in black hole mass. For NLS1s, we should consider other causes for the deviation from the correlation defined in equation (1). There are mainly several opinions about the origin about the narrow width of $H\beta$ in NLS1s. One is the small inclinations in NLS1s (Fig.1 in McLure & Dunlop 2002; Bian & Zhao 2002); the second is the long distance of BLRs emitting line of $H\beta$ in NLS1s; the third is their higher value of L/L_{Edd} because of their low central black hole masses. From Fig. 2, the smaller inclination in NLS1s is possible if we think NLS1s follow the correlation defined by equation (1). Nelson & Whittle (1996) showed in their Fig. 8 that the velocity dispersion from the [OIII] FWHM of the more radio luminous objects tend to be overestimated, which would make radio-loud AGNs deviate much from the correlation defined in equation (1). Tad-

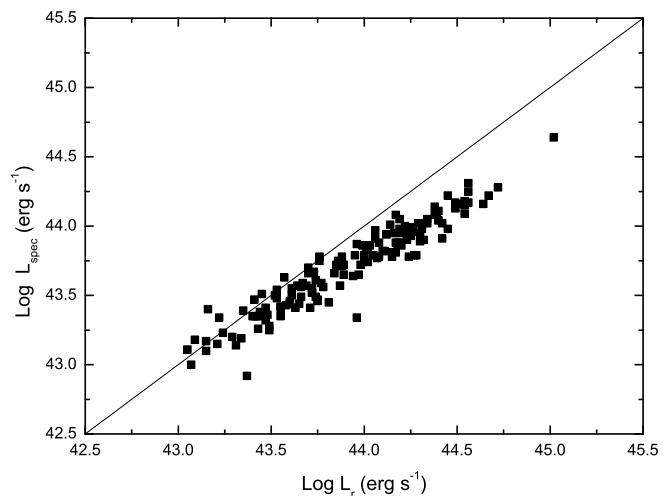


Figure 3. Monochromatic luminosity at 5100Å measured from the spectra of the SDSS NLS1s versus that from r^* band magnitude.

hunter et al. (2001) found that [OIII] of radio galaxy PKS 1549-79 is unusually broad and is blueshifted related to the low-ionization lines. They suggested there is an outflow in an inner NLRs. Recently Holt et al. (2003) investigated the intermediate resolution spectra ($\sim 4\text{\AA}$) of a radio source PKS 1345+12 and found there are three complex components on [OIII] emission line, which would affect the measurement of narrow [OIII] FWHM as a tracer of host velocity dispersion. For radio-loud AGNs, the [OIII] profile would be complex because of the interaction between radio jet and the interstellar medium (Gelderman et al. 1994). The research on the relation between narrow component of [OIII] line and the host velocity dispersion, especially for radio-loud AGNs, is needed.

4 CONCLUSION

The correlation between the central black hole mass and the bulge velocity dispersion was investigated in radio-quiet AGNs, radio-loud AGNs and NLS1s. The main conclusions can be summarized as follows:

- The radio-quiet AGNs follow the $M_{\text{bh}} - \sigma$ correlation defined by equation (1) founded in nearby inactive galaxies, while radio-loud AGNs and NLS1s seem not follow this correlation.
- Small inclination or overestimated bulge velocity dispersion can not account for the deviation of radio-loud AGNs from the correlation defined in equation (1). There are two possibility to explain this deviation in radio-loud AGNs. One is that the size of BLRs emitting $H\beta$ line is overestimated because of the overestimation of optical luminosity, the other is that the dynamics in BLRs and/or NLRs in radio-loud AGNs is different from that in radio-quiet AGNs.

- For NLS1s, small inclination may play a particular role in the deviation from the correlation defined in equation (1). We should consider the inclination effect in the black hole mass estimation using H β FWHM.

ACKNOWLEDGMENTS

We thank the anonymous referee for the valuable comments. This work has been supported by the NSFC (No. 10273007) and NSF of Jiangsu Provincial Education Department (No. 03KJB160060). The SDSS web site is <http://www.sdss.org/>. This research has made use of the NASA/IPAC Extragalactic Laboratory Database (NED), which is operated by the Jet Propulsion Laboratory, California Institute of Technology, under contract to NASA.

REFERENCES

- Bian W., Zhao Y., 2002, *A&A*, 395, 465
 Bian W., Zhao Y., 2003a, *PASJ*, 55, 599
 Bian W., Zhao Y., 2003b, *PASJ*, 55, 143
 Bian W., Zhao Y., 2003c, *MNRAS*, 343, 164
 Boroson T. A., 2003, *ApJ*, 585, 647
 Dunlop J.S., et al., 2003, *MNRAS*, 340, 1095
 Ferrarese L., Pogge R. W., Peterson B. M., Merritt D., Wandel A., Joseph C. L., 2001, *ApJ*, 555, L79
 Gebhardt K., et al., 2000, *ApJ*, 543, L5
 Gelderman R., Whittle M., 1994, *ApJS*, 91, 491
 Gu M., Cao X., Jiang D. R., 2001, *MNRAS*, 327, 1111
 Ho L.C., 1998, In “Observational Evidence for Black Holes in the Universe”, ed. S.K. Chakrabarti (Dordrecht: Kluwer) P157 (9803307)
 Holt J., Tadhunter C.N., Morganti R., 2003, *MNRAS*, 342, 227
 Jarvis M.J., McLure R.J., 2002, *MNRAS*, 336, L38
 Kaspi S., Smith P.S., Netzer H., Maoz D., Jannuzi B.T., Giveon U., 2000, *ApJ*, 533, 631
 McLure R. J., Dunlop J. S., 2001, *MNRAS*, 327, 199
 McLure R. J., Dunlop J. S., 2002, *MNRAS*, 331, 795
 Marziani Sulentic, J. W., Dultzin-Hacyan, D., Calvani, M., Moles, M., 1996, *ApJS*, 104, 37
 Nelson C. H., 2001, *ApJ*, 544, L91
 Nelson C. H., Whittle M., 1996, *ApJ*, 465, 96
 Schlegel D. J., Finkbeiner D. P., Davis M., 1998, *ApJ*, 500, 525
 Shields G.A., et al., 2003, *ApJ*, 583, 124
 Tadhunter C., Wills K., Morganti R., Oosterloo T., Dickson R., 2001, *MNRAS*, 327, 227
 Tremaine S., et al., 2002, *ApJ*, 574, 740
 Veilleux S., 1991, *ApJS*, 75, 383
 Veron-Cetty M. P., Veron P., 2001, *A&A*, 374, 92
 Vestergaard M., 2002, *ApJ*, 571, 733
 Wandel A., Peterson B.M., Malkan M.A., 1999, *ApJ*, 526, 579
 Wang T. G., Lu Y. J., 2001, *A&A*, 377, 52
 Willams R.J., Pogge R.W., Mathur S., 2003, *AJ*, 124, 3042

name (1)	z (2)	H β (3)	νL_ν (4)	M_{bh} (5)	$\sigma_{[\text{OIII}]}$ (6)
J000109.14-004121.5	0.417	1209	44.11	6.92	2.21
J000834.72+003156.2	0.263	1351	44.38	7.21	2.36
J001327.31+005232.0	0.363	1742	44.56	7.55	2.36
J002213.00-004832.7	0.214	1429	43.35	6.54	2.00
J002233.27-003448.6	0.504	1388	44.26	7.15	2.38
J002305.03-010743.5	0.166	1157	43.57	6.51	2.15
J002752.39+002615.8	0.205	1830	43.87	7.12	2.31
J003024.94+000254.5	0.288	743	43.72	6.23	2.25
J003238.20-010035.2	0.092	639	43.40	5.88	1.95
J003431.74-001312.7	0.381	1314	44.42	7.21	2.47
J003711.00+002128.0	0.235	617	43.85	6.16	2.35
J004052.14+000057.3	0.405	1278	44.49	7.24	2.60
J004338.54-005814.7	0.559	1122	44.45	7.10	2.39
J005446.16+004204.1	0.234	1225	43.78	6.71	2.11
J005921.37+004108.9	0.423	1625	44.08	7.16	2.48
J011357.93-011139.8	0.754	1842	44.72	7.72	2.60
J011703.58+000027.4	0.046	975	43.16	6.07	2.19
J011712.81-005817.5	0.486	1937	44.20	7.40	2.28
J011929.06-000839.7	0.090	900	43.44	6.20	2.34
J013046.16-000800.8	0.253	1648	43.63	6.86	2.44
J013521.68-004402.2	0.098	1181	43.45	6.44	2.48
J013842.05+004020.0	0.520	1035	44.24	6.88	2.48
J013940.99-010944.4	0.194	1091	43.71	6.55	2.26
J014234.41-011417.4	0.244	1607	43.96	7.07	2.07
J014412.77-000610.5	0.359	1041	43.66	6.48	2.28
J014542.78+005314.9	0.389	1255	43.86	6.78	2.41
J014559.45+003524.7	0.166	1075	43.43	6.35	2.49
J014644.82-004043.2	0.083	1164	43.22	6.27	2.03
J014951.66+002536.5	0.252	563	43.70	5.98	2.03
J015652.43-001222.0	0.163	1324	43.67	6.69	2.31
J020431.64+002400.5	0.171	1077	43.29	6.25	2.05
J021610.56+000538.4	0.384	1467	44.17	7.13	2.53
J021652.47-002335.3	0.304	854	44.06	6.59	2.37
J022205.37-004948.0	0.525	1571	44.54	7.45	2.26
J022756.28+005733.1	0.128	773	43.09	5.82	2.16
J022841.48+005208.6	0.186	990	43.64	6.42	2.31
J022923.43-000047.9	0.558	1386	44.40	7.25	2.30
J023057.39-010033.7	0.649	1947	44.56	7.65	2.26
J023211.83+000802.4	0.432	1746	44.00	7.16	2.45
J023414.58+005707.9	0.269	1381	43.75	6.79	2.24
J024037.89+001118.9	0.470	1789	44.19	7.32	2.21
J024651.91-005931.0	0.468	1504	45.02	7.75	2.11
J025501.19+001745.5	0.360	904	43.77	6.44	2.20
J030031.31+005357.2	0.198	1536	43.55	6.74	2.28
J030417.78+002827.4	0.044	1321	43.05	6.26	2.06
J030639.57+000343.2	0.107	1525	43.70	6.84	2.34
J031427.47-011152.4	0.387	1812	44.45	7.52	2.34
J031542.64+001228.7	0.207	870	43.73	6.37	2.60
J031630.79-010303.6	0.368	1226	44.12	6.94	2.39
J032255.49+001859.9	0.384	1621	44.49	7.45	2.48
J032337.65+003555.7	0.215	1490	44.15	7.13	2.55
J032606.75+011429.9	0.127	686	43.52	6.02	2.35
J033027.21+005433.7	0.443	1315	44.34	7.16	2.21
J033059.06+010952.1	0.557	1946	44.15	7.36	2.41
J033429.44+000611.0	0.347	1316	44.67	7.39	2.34
J033854.25+005339.7	0.279	1314	43.81	6.79	2.39
J033923.66-002310.3	0.369	1437	43.94	6.95	2.14
J034131.95-000933.0	0.223	897	43.53	6.26	2.39
J034326.51+003915.2	0.499	1315	44.32	7.15	2.24
J034430.03-005842.7	0.287	786	43.89	6.40	2.63
J094857.33+002225.5	0.584	1342	44.56	7.33	1.78
J095859.80+004718.9	0.235	1190	43.75	6.66	2.35
J100405.00-003253.4	0.289	582	44.14	6.31	2.58

Table 1. M_{bh} and $\sigma_{[\text{OIII}]}$ for NLS1s in SDSS. Col. (1): Object

J101314.86-005233.5	0.276	1578	44.29	7.28	2.63	J172007.96+561710.7	0.389	1221	43.84	6.74	2.35
J102059.72+010034.3	0.588	1715	44.64	7.60	2.38	J172206.04+565451.6	0.426	1579	44.39	7.36	2.45
J102450.52-002102.4	0.322	1382	44.17	7.08	2.13	J172756.86+581206.0	0.414	1742	43.96	7.14	2.43
J103031.41-001902.6	0.562	1787	44.22	7.34	2.37	J172800.67+545302.8	0.246	1583	44.00	7.08	2.48
J103222.58-000345.6	0.559	1707	44.19	7.28	2.04	J172823.61+630933.9	0.439	1750	44.30	7.38	2.43
J103457.29-010209.0	0.328	1394	44.49	7.31	2.19	J173404.85+542355.1	0.685	1163	44.42	7.11	2.42
J104132.35-003512.2	0.135	1316	43.15	6.33	2.03	J173721.14+550321.7	0.333	1256	44.22	7.04	2.24
J104210.03-001814.7	0.115	628	43.15	5.69	1.85	J232525.53+001136.9	0.491	1921	44.27	7.44	2.35
J104230.14+010223.7	0.116	1012	43.41	6.28	2.37	J233032.95+000026.4	0.123	956	43.55	6.33	2.29
J104331.51-010732.9	0.362	1756	44.05	7.20	2.35	J233149.49+000719.5	0.367	1708	44.25	7.32	2.53
J104449.28+000301.2	0.443	1176	44.07	6.87	2.51	J233853.83+004812.4	0.170	1011	43.48	6.32	2.04
J105932.52-004354.7	0.155	1451	43.37	6.56	2.39	J234050.53+010635.6	0.358	729	44.02	6.42	2.11
J110312.83+000012.5	0.276	1450	43.89	6.93	2.34	J234141.50-003806.7	0.319	1871	44.38	7.49	2.40
J111022.39-005544.5	0.257	1934	43.88	7.17	2.26	J234150.81-004329.2	0.251	1817	43.66	6.96	1.99
J111307.73+003210.4	0.346	976	44.16	6.77	2.36	J234216.74+000224.1	0.185	917	43.31	6.12	2.13
J113102.28-010122.0	0.242	1928	43.49	6.89	2.18	J234229.46-004731.6	0.316	1857	43.72	7.02	2.08
J113541.20+002235.4	0.175	1165	44.03	6.83	2.16	J234725.30-010643.7	0.182	1667	43.74	6.95	2.09
J115023.59+000839.1	0.127	1136	43.49	6.44	2.10						
J115306.95-004512.7	0.357	1102	43.98	6.75	2.20						
J115412.77+010133.4	0.490	945	44.31	6.85	2.45						
J115533.50+010730.6	0.197	1628	43.76	6.94	2.59						
J115755.47+001704.0	0.261	1762	43.97	7.16	2.44						
J115832.81+005139.2	0.591	1035	44.54	7.09	2.17						
J121415.17+005511.4	0.396	1981	44.30	7.49	2.32						
J122102.95-000733.7	0.366	517	44.17	6.23	2.38						
J122432.40-002731.4	0.157	1308	43.76	6.75	2.19						
J124519.73-005230.4	0.221	1730	43.53	6.83	2.20						
J125337.36-004809.6	0.427	1416	44.31	7.20	2.71						
J125943.59+010255.1	0.394	1459	44.30	7.22	2.77						
J130023.22-005429.8	0.122	1018	43.58	6.41	2.14						
J130707.71-002542.9	0.450	1475	44.18	7.15	2.51						
J130855.18+004504.1	0.429	1851	44.06	7.26	2.09						
J131108.48+003151.8	0.429	1642	44.54	7.49	2.66						
J132231.13-001124.5	0.173	1861	43.61	6.95	2.19						
J133031.41-002818.8	0.240	1216	43.60	6.58	2.26						
J133741.76-005548.2	0.279	873	43.69	6.35	2.51						
J135908.01+002732.0	0.257	1282	43.95	6.87	2.24						
J141234.68-003500.0	0.127	1098	43.21	6.21	2.08						
J141519.50-003021.6	0.135	1186	43.34	6.37	2.29						
J141820.33-005953.7	0.254	831	43.72	6.33	2.27						
J142441.21-000727.1	0.318	1201	44.23	7.01	2.22						
J143030.22-001115.1	0.103	1744	43.07	6.52	2.34						
J143230.99-005228.9	0.362	1559	43.99	7.06	2.72						
J143624.82-002905.3	0.325	1857	44.34	7.46	2.69						
J144735.25-003230.5	0.217	1105	43.65	6.53	2.01						
J144913.51+002406.9	0.441	944	44.08	6.69	2.45						
J144932.70+002236.3	0.081	1072	43.24	6.21	2.02						
J145123.02-000625.9	0.139	1122	43.43	6.38	2.18						
J145437.84-003706.6	0.576	1328	44.28	7.12	2.41						
J150629.23+003543.2	0.370	1861	44.19	7.36	2.18						
J151312.41+001937.5	0.159	1697	43.60	6.86	2.32						
J151956.57+001614.6	0.115	1716	43.61	6.88	2.17						
J153911.17+002600.8	0.265	539	44.10	6.22	2.31						
J164907.64+642422.3	0.184	759	43.47	6.07	2.20						
J165022.88+642136.1	0.407	1152	44.02	6.82	2.46						
J165338.69+634010.7	0.279	1848	44.25	7.39	2.55						
J165537.78+624739.0	0.597	1271	44.40	7.17	1.81						
J165633.87+641043.7	0.272	1139	43.74	6.61	2.42						
J165658.38+630051.1	0.169	1466	43.47	6.65	2.11						
J165905.45+633923.6	0.368	1359	44.20	7.09	2.41						
J170546.91+631059.1	0.119	1657	43.41	6.71	2.01						
J170812.29+601512.6	0.145	1094	43.42	6.36	2.27						
J170956.02+573225.5	0.522	1329	44.50	7.28	2.14						
J171033.21+584456.8	0.281	652	43.88	6.22	2.28						
J171207.44+584754.5	0.269	1708	44.18	7.27	2.41						
J171540.92+560655.0	0.297	1752	44.01	7.18	2.51						
J171829.01+573422.4	0.101	1322	43.55	6.61	2.35						

name (1)	RL/RQ (2)	z (3)	H β (4)	νL_ν (5)	M_{bh} (6)	$\sigma_{[\text{OIII}]}$ (7)
0044+030	SS	0.6232	5480	45.75	9.13	2.54
0050+124	RQ	0.0604	4460	44.47	8.29	2.81
0121-590	RQ	0.0460	6080	44.31	8.45	2.39
0349-146	SS	0.6162	9470	45.67	9.55	2.38
0403-132	FS	0.5705	4490	45.27	8.64	2.42
0405-123	FS	0.5725	4830	46.19	9.35	2.42
0414-060	SS	0.7750	14820	46.03	10.13	2.38
0454-220	SS	0.5334	6920	45.67	9.31	2.54
0710+118	SS	0.7700	19530	45.67	10.12	2.27
0742+318	FS	0.4610	7240	45.75	9.43	2.23
0838+133	SS	0.6808	3090	44.95	8.05	2.29
0850+440	RQ	0.6139	3080	45.55	8.49	2.62
0918+511	RQ	0.5563	4540	44.71	8.26	2.73
0923+392	FS	0.6948	8210	45.23	9.09	2.38
0953+414	RQ	0.2341	3010	45.35	8.49	2.44
0955+326	SS	0.5305	4730	45.79	9.06	2.59
1001+292	RQ	0.3297	2450	45.27	8.21	2.57
1007+417	SS	0.6123	2860	45.91	8.68	2.46
1049-005	RQ	0.3599	4510	45.39	8.81	2.38
1100+772	SS	0.3115	7840	45.43	9.34	2.38
1103-006	SS	0.4233	6600	45.39	9.12	2.44
1116+215	RQ	0.1765	3130	45.23	8.46	2.70
1136-374	RQ	0.0096	3780	42.99	7.13	2.21
1137+660	SS	0.6460	4950	45.75	9.03	2.31
1202+281	RQ	0.1653	5020	44.87	8.62	2.33
1211+143	RQ	0.0809	2320	44.71	7.88	2.24
1216+069	RQ	0.3313	5790	45.51	9.13	2.16
1226+023	FS	0.1575	3650	45.87	9.05	2.61
1253-055	FS	0.5362	21610	44.95	9.79	2.87
1302-102	FS	0.2784	3850	45.55	8.82	2.48
1351+640	RQ	0.0882	3670	44.75	8.30	2.54
1411+442	RQ	0.0896	2600	44.99	8.17	2.42
1415+253	RQ	0.0167	6200	43.39	7.84	2.30
1444+407	RQ	0.2673	2840	45.39	8.45	2.36
1512+370	SS	0.3707	9360	45.35	9.41	2.34
1538+477	RQ	0.7721	4920	46.19	9.28	2.46
1545+210	SS	0.2643	6730	44.83	8.81	2.41
1618+177	SS	0.5551	11530	45.59	9.69	2.47
1637+574	FS	0.7506	4620	45.71	8.90	2.46
1641+399	FS	0.5928	4870	45.75	9.04	2.50
1704+608	SS	0.3721	6990	45.71	9.41	2.27
1928+738	FS	0.3021	3120	45.23	8.40	2.22
2041-109	RQ	0.0344	3090	44.43	7.95	2.38
2135-147	SS	0.2003	7570	45.03	9.08	2.19
2141+175	FS	0.2111	4320	44.99	8.56	2.68
2201+315	FS	0.2950	3410	45.31	8.54	2.46
2251+113	SS	0.3255	4540	45.31	8.78	2.41
2308+098	SS	0.4333	11330	45.51	9.67	2.46

Table 2. M_{bh} and $\sigma_{[\text{OIII}]}$ for AGNs. Col. (1): Object name. Col. (2):RQ denotes Radio quiet objects, SS denotes steep-spectrum objects, and FS denotes flat-spectrum objects. Col. (3): Redshift. Col. (4): FWHM of the broad H β line in units of km s $^{-1}$. Col. (5): log of continuum luminosity at 5100 \AA rest wavelength in units of erg s $^{-1}$. Col. (6): log of the black hole mass in units of solar mass. Col. (7): log of the bulge velocity dispersion derived from FWHM of [OIII] line in units of m s $^{-1}$.

Type	$\log(M_{\text{H}\beta}/M_{[\text{OIII}]})$	SD
RL(Marziani)	0.51 ± 0.13	0.73
FS(Marziani)	0.13 ± 0.2	0.70
SS(Marziani)	0.74 ± 0.16	0.66
RL(Shields)	0.59 ± 0.10	0.61
RQ(Marziani)	-0.36 ± 0.19	0.81
RQ(Shields)	0.17 ± 0.10	0.68
RQ(Boroson)	0.08 ± 0.07	0.75
NLS1s(Wang)	-0.84 ± 0.11	0.79
NLS1s(Williams)	-1.29 ± 0.06	0.75

Table 3. The distributions of $\log(M_{\text{H}\beta}/M_{[\text{OIII}]})$ for different type of AGNs. RL(Marziani): Radio-loud AGNs in Marziani et al. (1996); FS(Marziani): Flat-spectrum AGNs in Marziani et al. (1996); SS(Marziani): Steep-spectrum AGNs in Marziani et al. (1996); RQ(Marziani): Radio-quiet AGNs in Marziani et al. (1996); RL(Shields): Radio-loud AGNs in Shields et al. (2003); RQ(Shields): Radio-quiet AGNs in Shields et al. (2003); RQ AGNs(Boroson): Radio-quiet AGNs in Boroson (2003); NLS1s(Wang): NLS1s in Wang & Lu (2001); NLS1s(Williams): NLS1s in Williams et al.(2003).